10

Magnetic Refrigeration Technology at Room Temperature

Houssem Rafik El-Hana Bouchekara[1,2] and Mouaaz Nahas[1]
[1]*Department of Electrical Engineering, College of Engineering and Islamic Architecture, Umm Al-Qura University, Makkah,*
[2]*Electrical Laboratory of Constantine "LEC", Department of Electrical Engineering, Mentouri University – Constantine, Constantine,*
[1]*Saudi Arabia*
[2]*Algeria*

1. Introduction

Modern society largely depends on readily available refrigeration methods. Up till now, the conventional vapor compression refrigerators have been mainly used for refrigeration applications. Nonetheless, the conventional refrigerators – based on gas compression and expansion – are not very efficient because the refrigeration accounts for 25% of residential and 15% of commercial power consumption (Tishin, 1999). Moreover, using gases such as chlorofluorocarbons (CFCs) and hydrochlorofluorocarbons (HCFCs) have detrimental effects on our environment. Recently, the development of new technologies – such as magnetic refrigeration – has brought an alternative to the conventional gas compression technique (Manh, 2007).

The magnetic refrigeration at room temperature is an emerging technology that has attracted the interest of researchers around the world (Bouchekara, 2008). Such a technology applies the magnetocaloric effect which was first discovered by Warburg (Bohigas, 2000; Zimm, 2007). In 1881, Warburg noticed an increase of temperature when an iron sample was brought into a magnetic field and a decrease of temperature when the sample was removed out of it. Thus, the magnetocaloric effect is an intrinsic property of magnetic materials; where it is defined as the response of a solid to an applied magnetic field which appears as a change in its temperature (Bohigas, 2000; Zimm, 2007). Such materials are called magnetocaloric materials. The magnetocaloric effect is present in all transition metals and lanthanide-series elements, which may have ferromagnetic behaviour. When a magnetic field is applied, the magnetic moments of these metals tend to align parralel to it, and the thermal energy released in this process produces the heating of the sample. The magnetic moments become randomly oriented when the magnetic field is removed, thus the ferromagnet cools down (Gschneidner, 1998).

The ultimate goal of this technology would be to develop a standard refrigerator for home use. The use of magnetic refrigeration has the potential to reduce operating and maintenance costs when compared to the conventional method of compressor-based refrigeration. By eliminating the high capital cost of the compressor and the high cost of

electricity to operate the compressor, magnetic refrigeration can efficiently (and economically) replace compressor-based refrigeration technology. Some potential advantages of the magnetic refrigeration technology over the compressor-based refrigeration are: [1] green technology (no toxic or antagonistic gas emission); [2] noiseless technology (no compressor); [3] higher energy efficiency; [4] simple design of machines; [5] low maintenance cost; and [6] low (atmospheric) pressure (this is an advantage in certain applications such as in air-conditioning and refrigeration units in automobiles).

This chapter is concerned with the magnetic refrigeration technology form the material-level to the system-level. It provides a detailed review of the magnetic refrigeration prototypes available until now. The operational principle of this technology is explained in depth by making analogy between this technology and the conventional one. The chapter also investigates the study of the magnetocaloric materials using the molecular field theory. The thermal and magnetic study of the magnetic refrigeration process using the finite difference method (FDM) is also explained and are presented and discussed in detail.

The chapter is organized as follows. Section 2 introduces the magnetocaloric effect and its application to produce cold. It also introduces active magnetic regenerative refrigeration. Section 3 reviews ten various magnetic refrigeration systems and highlights their pros and cons. In Section 4 and 5, the thermal and magnetic study of the magnetic refrigeration process using the finite difference method are explained and the results from the thermal study are also presented and discussed in detail. Finally, the conclusions are drawn in Section 6.

2. The magnetocaloric effect

2.1 Definition

The magnetocaloric effect (MCE) is an intrinsic property of magnetic materials; it consists of absorbing or emitting heat by the action of an external magnetic field (Tishin, 1999). This results in warming or cooling (both reversible) the material as shown in Fig. 1.

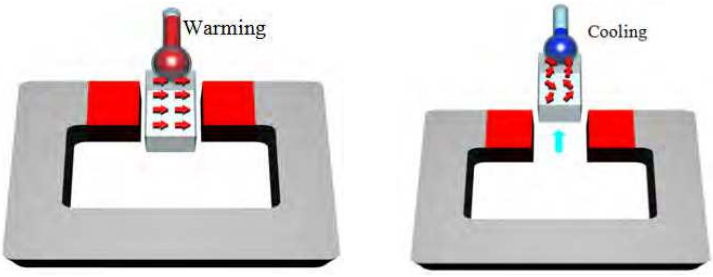

Fig. 1. Magnetocaloric effect (the arrows symbolize the direction of the magnetic moments).

2.2 Thermodynamic approach

The absolute entropy, which is a function of temperature and induction in the magnetocaloric material is a combination of the magnetic entropy, the entropy of the lattice and the entropy of the conduction electrons (assumed negligible). It is given by the following equation:

$$S(T,B) = S_m + S_l \tag{1}$$

where S (J K^{-1}) is the entropy (subscripts m and l are respectively for magnetic and lattice entropies), T (K) is the temperature and B (T) is the magnetic filed induction.

In magnetocaloric materials, a significant variation of the entropy can be observed by the application or removal of an external magnetic field. For a given material, MCE depends only on its initial temperature and the magnetic field. The MCE can be interpreted as the isothermal entropy change or the adiabatic temperature change.

The separation of entropy into three terms given in (1) is valid only for second order phase transition materials characterized by a smooth variation of the magnetization as a function of temperature. For first order transitions (abrupt change of magnetization around the transition temperature), this separation is not accurate (Kitanovski, 2005). For most applications, it is sufficient to work with the total entropy which - in its differential form - can be given as:

$$dS(T,B) = \left(\frac{\partial S}{\partial T}\right)_B dT + \left(\frac{\partial S}{\partial B}\right)_T dB \tag{2}$$

The specific heat capacity C_B (J m^{-3} K) of the material is given as:

$$C_B = \left(\frac{\partial S}{\partial T}\right)_B T \tag{3}$$

This gives:

$$\left(\frac{\partial S}{\partial T}\right)_B = \frac{C_B}{T} \tag{4}$$

From (2) and (4) we can write:

$$dS(T,B) = \frac{C_B}{T} dT + \left(\frac{\partial S}{\partial B}\right)_T dB \tag{5}$$

In the case of an adiabatic process (no entropy change $\Delta S = 0$) the temperature variation can be written as:

$$dT = -\frac{T}{C_B}\left(\frac{\partial S}{\partial B}\right)_T dB \tag{6}$$

Using the Maxwell relation given as:

$$\left(\frac{\partial S}{\partial B}\right)_T = \left(\frac{\partial M}{\partial T}\right)_B \tag{7}$$

where M (A m^{-1}) is the magnetization.

We can write:

$$dT = -\frac{T}{C_B}\left(\frac{\partial M}{\partial T}\right)_B dB \tag{8}$$

The magnetocaloric effect (the adiabatic variation in temperature) can then be expressed as follows:

$$\Delta T_{ad} = -\int_{B_i}^{B_f} \frac{T}{C_B}\left(\frac{\partial M}{\partial T}\right)_B dB = MCE \tag{9}$$

In the case of an isothermal process, the temperature does not change during the magnetization and we can express the entropy as:

$$dS(T,B) = \left(\frac{\partial S}{\partial B}\right)_T dB \tag{10}$$

Using the Maxwell relation given by (7), the magnetic entropy change can be expressed as:

$$\Delta S = \int_{B_i}^{B_f} \left(\frac{\partial M}{\partial T}\right)_B dB \tag{11}$$

and the heat saved in this way is transferred to the lattice thermal motion.

2.3 Theoretical approach of MCE: molecular field theory

The theoretical calculation of the MCE is based on the model of Weiss (MFT: Molecular Field Theory) and the thermodynamic relations (Huang, 2004). To interpret quantitatively the ferromagnetism, Weiss proposed a phenomenological model in which the action of the applied magnetic field **B** was increased from that of an additional magnetic field proportional to the volume magnetization density B_v as:

$$B_v = \lambda \mu_0 M \tag{12}$$

The energy of a magnetic moment is then:

$$E = -\mu\left(B + B_v\right) \tag{13}$$

The magnetic moments will tend to move in the direction of this new field. Adapting the classical Weiss-Langevin classical calculations to a system of quantum magnetic moments, one finds:

$$M(x) = n g_J \mu_B B_J(x) \tag{14}$$

where:

$$x = \frac{J g_J \mu_B \left(B + \lambda \mu_0 M(x)\right)}{k_B T} \tag{15}$$

and

$$B_J(x) = \frac{2J+1}{2J}\coth\left(\frac{2J+1}{2J}x\right) - \frac{1}{2J}\coth\left(\frac{1}{2J}x\right) \tag{16}$$

where: J (N m s) is the total angular momentum, n (mol^{-1}) is the Avogadro number, g_J is the Landé factor, μ_B (J T^{-1}) is the Bohr magnetron, k_B (J K-1) is the Boltzmann constant, $B_J(x)$ is the Brillouin function, λ is the Weiss molecular field coefficient and μ_0 (T m A-1) is the Permeability of vacuum.

The magnetic entropy is given by the relationship of Smart (Allab, 2008):

$$S_m(x) = R\left(\ln\left(\sinh\left(\frac{2J+1}{2J}x\right)\Big/\sinh\left(\frac{1}{2J}x\right)\right) - xB_J(x)\right) \tag{17}$$

The lattice contribution can be obtained using the Debye model of phonons (Allab, 2008). It is given by the following equation:

$$S_r = R\left(-3\ln\left(1-e^{\frac{-T_D}{T}}\right) + 12\left(\frac{T}{T_D}\right)^3 \int_0^{\frac{T_D}{T}} \frac{y^3}{e^y-1}dy\right) \tag{18}$$

where: T_D (K) is the Temperature of Debye and R (J K^{-1} mol^{-1}) is the universal gas constant.

2.3.1 Application of MFT to gadolinium (Gd)

In this section the theoretical study based on the MFT developed in the previous section is applied to the gadolinium. Table 1 gives the parameters used to calculate the magnetocaloric properties.

J	n	g_J	μ_B	k_B	μ_0	T_C	T_D
3.5	6.023 10^{23}	2	9.2740154 10^{-24}	1.380662 10^{-23}	4π 10^{-7}	293	184

Table 1. Parameters used for applying MFT to the gadolinium.

The numerical solution of equations (14), (15) and (16) allows getting the isotherms of magnetization and its evolution as a function of temperature calculated by the method of Weiss as shown in Fig. 2 (a) and Fig. 2 (b). Fig. 2 (c) represents the total heat capacity calculated from the equation (3) for different levels of induction. The magnetic entropy and its variation with temperature are shown respectively in Fig. 2 (d) and Fig. 2 (e). Finally, Fig. 2 (f) shows the magnetocaloric effect calculated by the MFT.

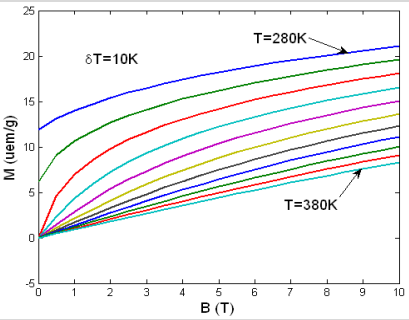

(a) Variation of magnetization versus the Magnetic field.

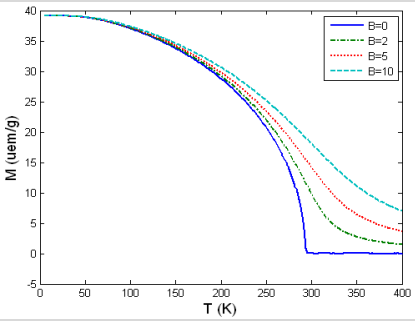

(b) Variation of magnetization versus the temperature.

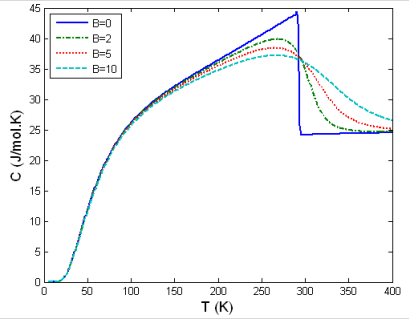

(c) Evolution of the total heat capacity as a function of temperature.

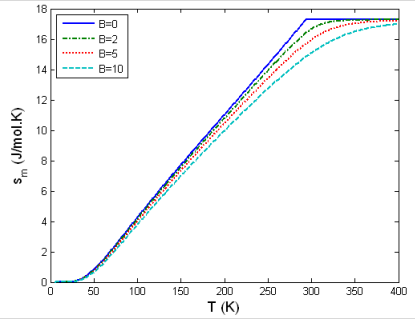

(d) Magnetic entropy.

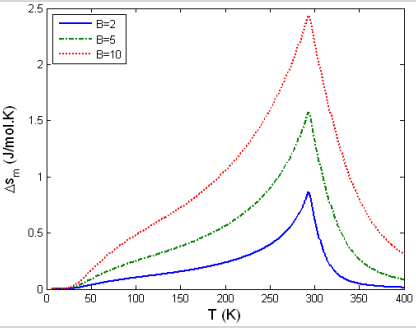

(e) Variation of the magnetic entropy.

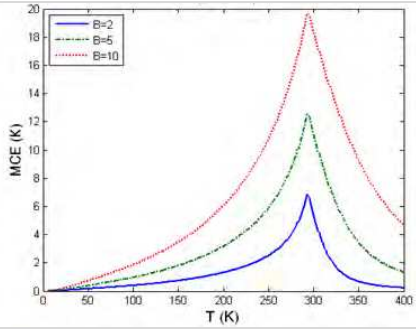

(f) MCE of Gd calculated by the MFT.

Fig. 2. Results of the theoretical study applied to Gd.

2.4 Application of MCE to produce cold

The magnetic cycles are generally composed of the process of magnetization and demagnetization, in which heat is discharged or absorbed in four steps as depicted by Fig. 3. From thermodynamic point of view, the magnetic cooling can be realized by: Carnot, Stirling, Ericsson and Brayton, where the Ericsson and Brayton cycles are believed to be the most suitable for such medium or room temperature cooling. Such cycles are predisposed to yield high cooling efficiency of the magnetic materials (Bouchekara, 2008).

Fig. 3(a) shows the conventional gas compression process that is driven by continuously repeating the four different basic processes shown while Fig. 3 (b) shows the magnetic refrigeration cycle comparison. The steps of the magnetic refrigeration process are analogous to those of the conventional refrigeration. By comparing (a) with (b) in Fig. 3, one can see that the compression and expansion are replaced by adiabatic magnetization and demagnetization, respectively. These processes change the temperature of the material and heat may be extracted and injected just as in the conventional process.

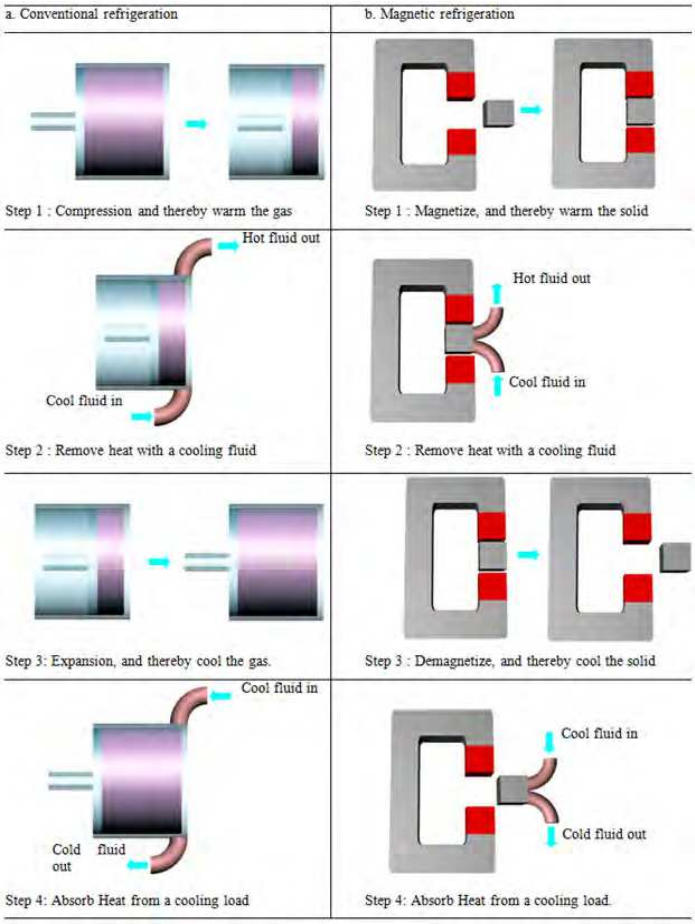

Fig. 3. Analogy between magnetic refrigeration and conventional refrigeration.

2.5 The Active Magnetic Regenerative Refrigeration (AMRR)

The direct exploitation of the giant MCE around the room temperature is limited by the fact that existing MCE materials do not achieve high temperature differences (Lebouc, 2005). For example, a sample of gadolinium around room temperature produces an MCE of approximately 10 K in a magnetic field of 5 T.

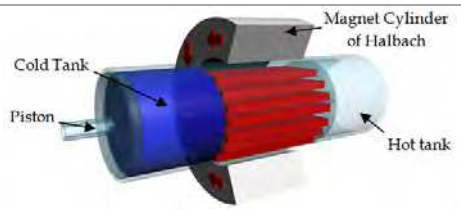

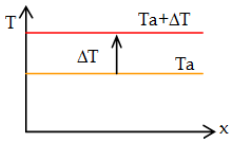

Step 1: Magnetization of the material from an initial state where the entire system is at temperature T_a. Each point of the regenerator material sees its temperature increase by ΔT following the application of the magnetic field.

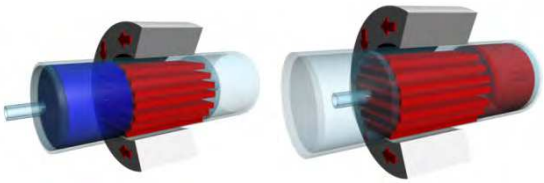

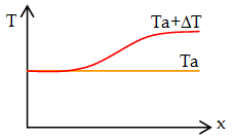

Step 2: Flow of the fluid from the cold source to the hot source. The heat produced by the magnetization step is removed by the fluid flowing from the cold source T_c to the hot source T_h. This creates a temperature gradient along the bed.

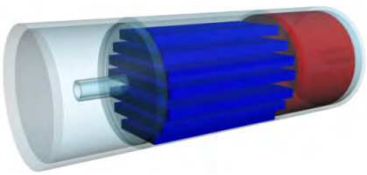

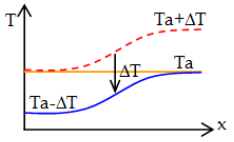

Step 3: demagnetization of the material. The temperature of Each point of the regenerator decreases by Δ T due to the demagnetization.

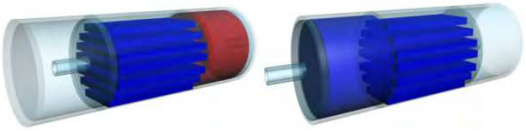

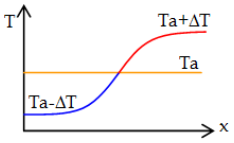

Step 4: Flow of fluid from the hot source to cold source. The flow of the fluid from the hot source T_h to the cold source T_f transfers its heat to the regenerator. The temperature gradient is amplified.

Fig. 4. Representation of AMRR cycle and temperature profile along the MCE material.

Since the gadolinium is considered as one of the best magnetocaloric materials currently available (Lebouc, 2005), the MCE corresponds to the absolute maximum value that can be obtained between the hot tank and cold tank. Thus it is obviously hard to imagine the exploitation of the MCE in most refrigeration applications (Engelbrecht, 2005).

This technical barrier has been overcome by the application of the Active Magnetic Regenerative Refrigeration (AMRR) (Engelbrecht, 2005; Lebouc, 2005; Tura, 2002). Regeneration in magnetic refrigeration systems allows the heat rejected by the network in any step of the cycle to be restored and returned to the network in another step in the same cycle (Yu, 2003). Thus, the capacity used for cooling the network load can be used effectively to increase the actual change of entropy and the obtained temperature difference (Yu, 2003).

AMRR cycles are illustrated in Fig. 4. The regenerative bed consists of plates of MCE material that initially have a quasi-linear temperature profile between the hot and cold tanks.

The bed itself acts as a regenerator. The different solid parts of the regenerator are connected by the fluid, so the heat does not need to be transferred between two solid parts separated, but on the same block.

Each particle of the bed undergoes a regenerative Brayton cycle and the entire bed undergoes a cascade Brayton cycle (Yu, 2003). This cycle is repeated 'n' times and the ΔT generated is amplified at each cycle to reach the temperatures limits of hot and cold sources (steady state). This ΔT is higher than the adiabatic temperature change of refrigerant material (MCE). In addition, the regenerator bed can be achieved by superposing different materials of different composition to expand the temperature's range of variation and thus to extend the utilization range of the system.

3. Magnetic refrigeration systems

Since the first magnetic refrigeration system manufactured by Brown in 1976, many researchers around the world have paid considerable attention to the magnetic refrigeration around room temperature and consecutively developed some interesting systems (Bouchekara, 2008) (Yu, 2010) (Bjørk, 2010). This section reviews – in detail – some of the magnetic refrigeration systems available until now.

3.1 The magnetic system of Brown

The system of Brown is a rotating system and employs an Ericsson cycle (Yu, 2003). The magnetic field is produced by an electromagnet (water cooled) with a maximum magnetic field of 7 T. The MCE material used is the Gd in the form of plates with 1 mm thickness, separated by stainless steel wires with 1 mm intervals to allow the regenerator fluid to flow vertically. The fluid is composed of 80% of water and 20% of alcohol. Without load and after 50 cycles, the temperatures reached were 46 ° C for the heat source and -1 ° C for the cold source, thus $\Delta T = 47°C$. However, the cooling power obtained was not rely important, this is due to the large ΔT obtained. Moreover, the cycle can operate only at low frequencies; the temperature gradient is reduced because both warm and cold sides have time to interact.

3.2 The magnetic system of Steyert

An alternative system with a rotating refrigerant, implementing a Brayton's cycle has been designed by Steyert (Yu, 2003). In this system, the porous magnetocaloric material has a form of rings. This wheel (the regenerator with a ring form) rotates through a first area of

low magnetic field and a second area of high magnetic field as shown in Fig. 5. The exchange fluid enters the wheel (regenerator) at the temperature T_{hot} and exits at the temperature T_{cold}, having transferred its heat to the coolant located in the area of weak field. After receiving the heat of the load to cool Q_{cold} the fluid enters the wheel again at a temperature $T_{cold} + \Delta$ due to heat exchange with the wheel which is at this instant at the temperature $T_{hot} + \Delta$. The temperature of the fluid increases to $T_{hot} + \Delta$. Finally, the fluid transfers heat Q_{hot} to the reservoir of the hot source completing one cycle at the same time. Fig. 5 describes schematically the magnetic system of Steyert.

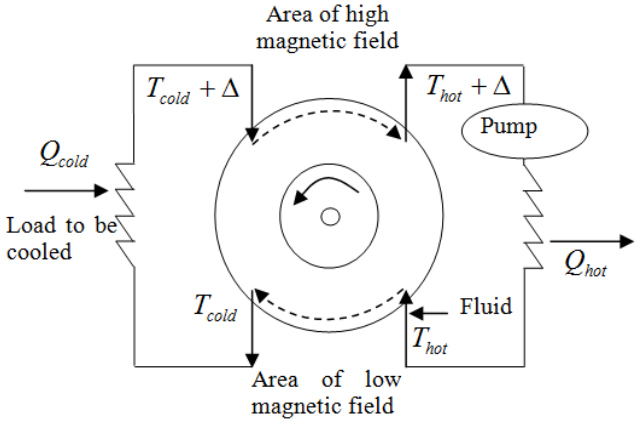

Fig. 5. Schematic representation of the Steyert's magnetic system.

3.3 The magnetic system of Kirol

This system was designed by Kirol (Yu, 2003) on the principle of a rotating machine and Ericsson's cycle. The magnetic field is produced by permanent magnets NdFeB and reaches a maximum value of 0.9 T in the air-gap. The refrigerant rotor is composed of a flat disk of 270 g of gadolinium as magnetocaloric material. During one rotation of the rotor, the four thermodynamic cycles are operated and a ΔT of 11 K is obtained.

3.4 The Spanish device

The device shown in Fig. 6 was developed by the team of the Polytechnic University of Catalonia in Barcelona (Allab, 2008). The magnetocaloric material is a ribbon of gadolinium (Gd 99.9%) fixed on a plastic disc and immersed in a fluid (olive oil). The magnetic cycle of magnetization / demagnetization is provided by the rotation of the plastic disc and its interaction with a magnet. The temperature span is obtained respectively: 1.6 and 5 K for a magnetic field of 0.3 T and 0.95 T. This corresponds to 2.5 times the MCE of Gd. Even if obtained performances of this system were weak, this device is the first that has shown the feasibility of magnetic refrigeration with fields accessible by permanent magnets.

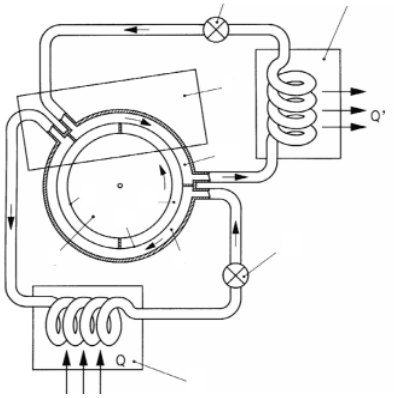

Fig. 6. The Magnetic device made in Spain (Bohigas, 2000).

3.5 Japanese system

Okamura et al. have constructed a magnetic refrigeration system, as shown in Fig. 7-a (Okamura, 2006). The yoke has an outer diameter of 27 cm and a length of 40 cm. The magnetic field is produced by rotating permanent magnets, producing a maximum field of 0.77 T. The bed regenerator is composed of 4 blocks. Each block is composed of a different alloy GdDy (sphere shaped) to enhance the range of variation of temperature. The fluid circulation is ensured by a pump and a rotary valve. The power obtained is about 60 W. The initial system has been improved as shown in Fig. 7-b (Okamura, 2007). The stator used was a laminated yoke and the magnetic field source was improved (the maximum field is 0.9 T). This helped to obtain a power of 100 W (using Gd as MCE material).

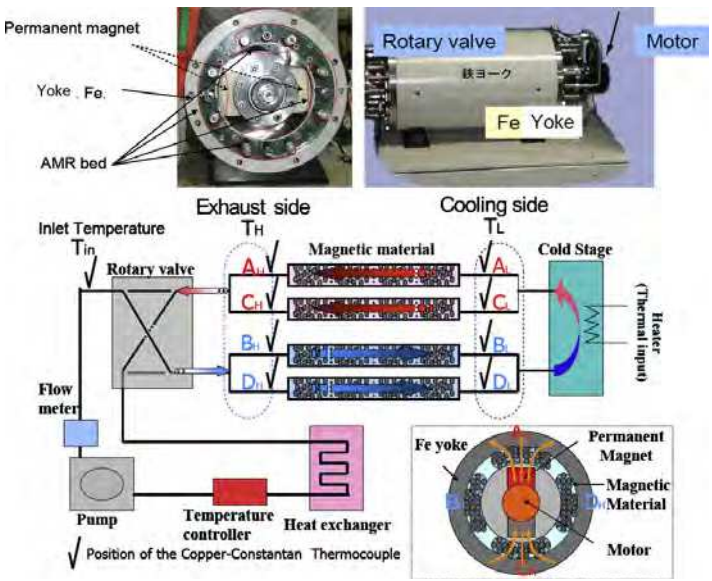

(a)

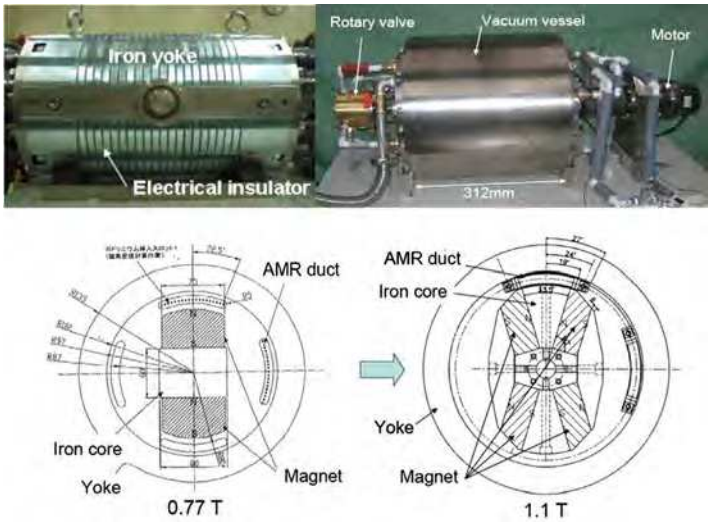

(b)

Fig. 7. The Japanese Device: (a) The initial one, (b) The improved one (Hirano et al., 2007; Okamura et al., 2006, 2007).

3.6 The magnetic system of Zimm

The ACM (Astronautics Corporation in Madison) has led many researches on magnetic refrigeration and achieved several patents in this field (Engelbrecht, 2005). In this corporation, an AMRR system was designed; it consists of a wheel with 6-bed regenerators composed of gadolinium powder. This wheel is rotating inside an area of high magnetic field of 1.5 T. The regenerative beds exchange with the fluid. The flow of the fluid is adjusted according to the relative position of each bed inside the magnetic field. Fig. 8 shows the photography of this prototype.

For cycles rotating with a frequency varying from 0.16 to 2 Hz and water rate flows varying from 0.4 to 0.8 l/min, the temperature spans obtained between the heat source and the cold source are from 4 to 20°C and the cooling power values are from 50 to 100W.

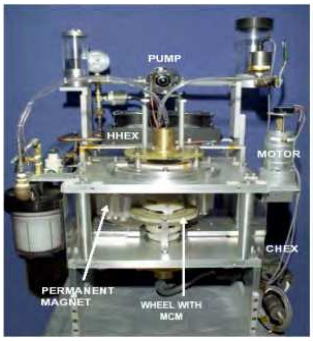

Fig. 8. ACM prototype (Zimm, 2002).

3.7 Canadian system

At the University of Victoria in Canada, Tura and Rowe (2007) constructed a magnetic refrigerator containing permanent magnets for a testing of all sorts of magnetic refrigerants in different configurations. This machine is shown in Fig. 9. A nested Halbach array of NbFeB permanent magnets was applied and led to a magnetic field of 0.1-1.47 T strength. Water was the heat transfer fluid with a heat rejection temperature range of 253-311 K, and the operation frequency was between 0 Hz and 4 Hz. The prototype showed cylindrical magnetocaloric regenerators (with a porosity of 57%) whose volume, diameter and length were 20 cm^3, 16 mm, and 110 mm, respectively. The void in the regenerator of the hot heat exchanger and the cold heat exchanger was 0.83 cm^3 and 0.4 cm^3, and the parallel flow paths in the heat exchangers were optimized with a computational fluid dynamics (CFD) approach. The system which is designed to be flexible showed many advantages: for example, a simple design, easy accessibility to all the components and very low heat leakages. This machine reached a maximum temperature span of 13.2 K (Yu, 2010).

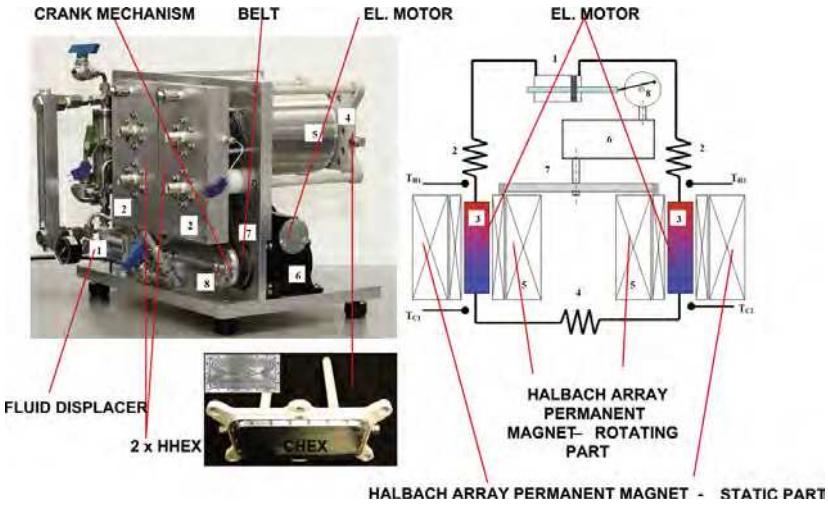

Fig. 9. Rotary magnetic refrigerator with permanent magnets as presented by researchers of the University of Victoria in Canada (Tura and Rowe, 2007).

3.8 Cooltech systems

The company Cooltech Applications in France built a rotary magnetic refrigerator composed of eight pieces of supporting discs positioned in synthetic material (see Fig. 10), which were mechanically stable and thermally isolated (Vasile and Muller, 2005, 2006).. These inserts were interchangeable for the test of different magnetocaloric materials, different sensors for temperature, pressure, air velocity, hydrometry and electrical power. Each insert was packed with 165 g Gd. The rotating axes were made of stainless steel, where four pieces of NdFeB permanent magnets were rotating to provide a magnetic field of 1 T. However, the authors reported on a new type (open Halbach) magnetic assembly, which yielded a magnetic field between 1 to 2.4 T. The flow of fluid was controlled to improve the cooling capacity, which was obtained in the range of 100W to 360 W (Yu, 2010).

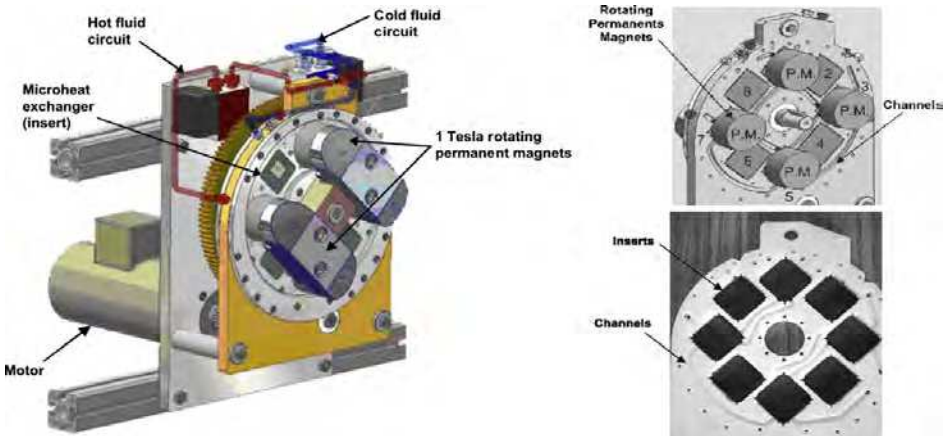

Fig. 10. 3D structure form of the Cooltech magnetic refrigerator, some details in further pictures, photography of the assembly and the open Halbach type of magnet (Vasile and Muller, 2005, 2006).

A rotary magnetic refrigerator prototype was developed in collaboration between the National Institute of Applied Sciences INSA of Strasbourg and the company Cooltech Applications in France (Muller et al., 2007). The system was composed by a rotary magnet assembly and of four static blocks of magnetocaloric material performed by gadolinium. The maximum magnetic field was 1.3 T and water was the working fluid. Unfortunately, there is no more information available. However, from Fig. 11, one may easily verify the manner how the magnetic field is produced in the magnetocaloric material (Yu, 2010).

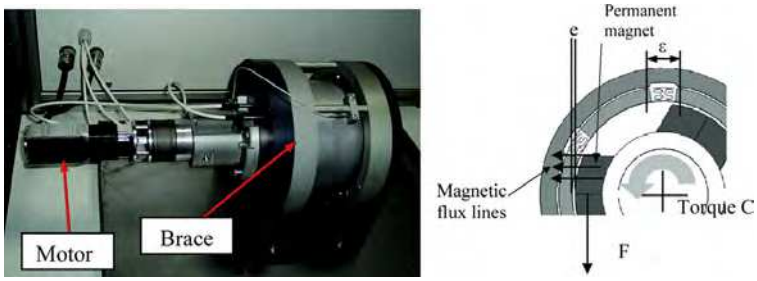

Fig. 11. A rotary magnetic refrigerator of the joint collaboration action between Cooltech Applications and INSA in France (Muller et al., 2007).

In France at Cooltech Applications, Bour et al. built a reciprocating prototype as it is shown in Fig. 12. The AMR bed was composed of 37 parallel plates of Gadolinium of 0.6 mm thickness, showing a spacing of the heat transfer fluid channels of 0.1 mm and 0.2 mm, respectively. The Halbach arrays, which produced a magnetic field intensity between 0.8 T and 1.1 T in the air gap, consisted of an assembly of three sets of NdFeB magnets of 50 mm thickness. The French experts obtained experimentally the evolutions of the average temperatures at the hot end and the cold end reservoirs for different initial temperatures and operation frequencies. The device led to a maximum temperature span of 16.1 K (Yu, 2010).

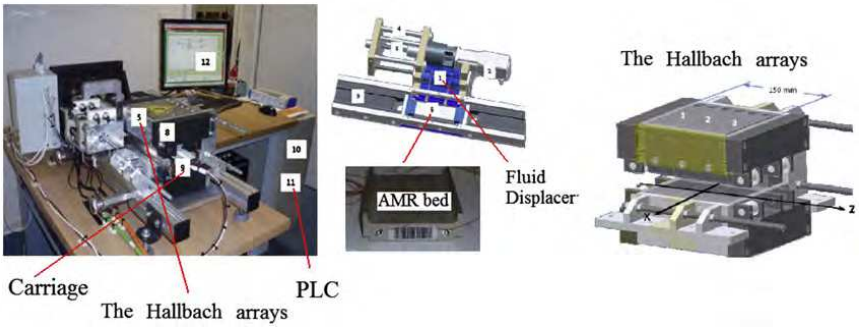

Fig. 12. The reciprocating prototype built at Cooltech Application in France (Bour et al., 2009).

3.9 The G2Elab prototypes

The first device constructed at G2Elab (Grenoble Electrical Engineering Laboratory) is an alternating device type as shown in Fig. 13. The regenerator is composed of parallel plates of gadolinium with 1 mm in thickness and 50 mm in length. The magnetic field is produced by a permanent magnet (Halbach cylinder) creating a magnetic field of 0.8 T. The fluid used is water. Its circulation is ensured by a peristaltic pump operating in both directions (Clot, 2002). The pneumatic actuator produces the movement of the refrigerant blocs and provides magnetization / demagnetization phases. The controller is programmed to manage the Halbach cylinder and the flow of fluid to perform the four phases of the cycle. The system is closed and there is no exchange with the outside. It was designed to study the Active Magnetic Regenerative Refrigeration (AMRR) cycles and exploit different materials.

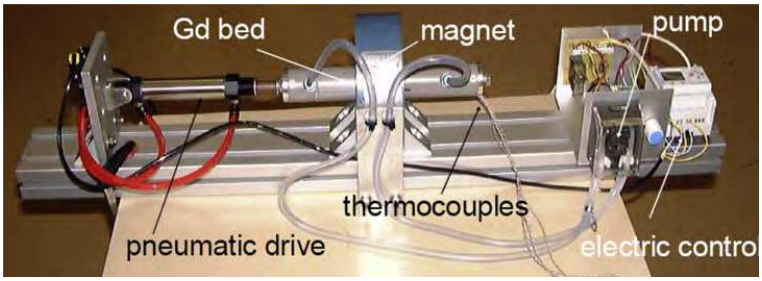

Fig. 13. The G2Elab first device (Clot, 2002).

A second prototype was developed at G2Elab (Allab, 2008), (Bouchekara, 2008), (Dupuis, 2009). This structure is quite similar to a rotating machine. It is also similar to some existing prototypes (Okamura, 2005, 2007). It consists of a permanent magnet which forms the rotor and of a stator made of magnetic yoke and four refrigerant beds (see Fig. 14).

The yoke is composed of four poles which are aimed to better conduct the magnetic flux within the refrigerant bed. The magnetization and demagnetization phases are obtained by a simple rotation of the permanent magnet. The beds undergo an active magnetic regenerative refrigeration AMRR cycle and operate two by two in the opposite way.

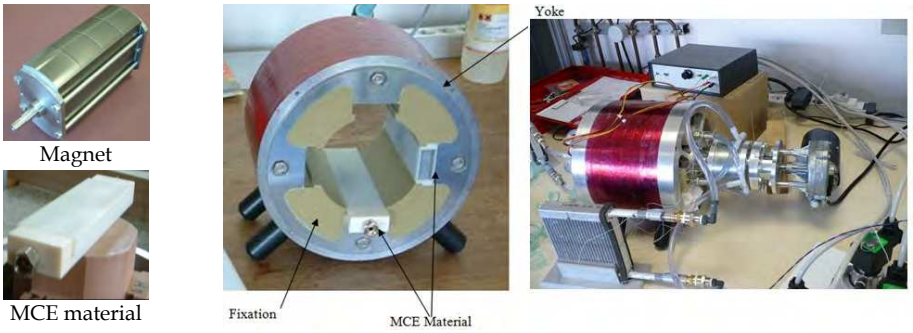

Fig. 14. The second prototype of the G2Elab, Components of the prototype (left) and the Prototype in its actual environment (right) (Bouchekara, 2008).

3.10 The Slovenian system

An interesting prototype of a rotary magnetic refrigerator (Tusek et al., 2009) has been built on the basis of permanent magnets at the University of Ljubljana in Slovenia. Their rotary magnetic refrigerator consisted of a rotating drum (cylinder) that rotated around an internally positioned stationary soft iron core and externally positioned stationary permanent magnets. As shown in Fig. 15, the magnetic structure was composed of four NdFeB permanent magnets and low carbon 1010 steel used as a soft ferromagnetic material, and two magnetic circuits existed to allow the rotary movement of the AMR's. After optimization of the magnet structure geometry, a range of magnetic field intensities from 0.05 T to 0.98 T was obtained in the air gaps. There were 34 AMR's in the rotary drum and each AMR had the dimensions 10 mm × 10 mm × 50 mm. Gd plates, with a thickness of 0.3 mm, were filled in the AMR's and the total mass of Gd was approximately 600 g. The prototype could operate up to a frequency of 4 Hz. This reference mainly focused on the experience in development of such a rotary magnetic refrigeration prototype and no experimental results were reported. However, first predictions according to the researchers are that approximately a 7 K temperature difference will be achieved (Yu, 2010).

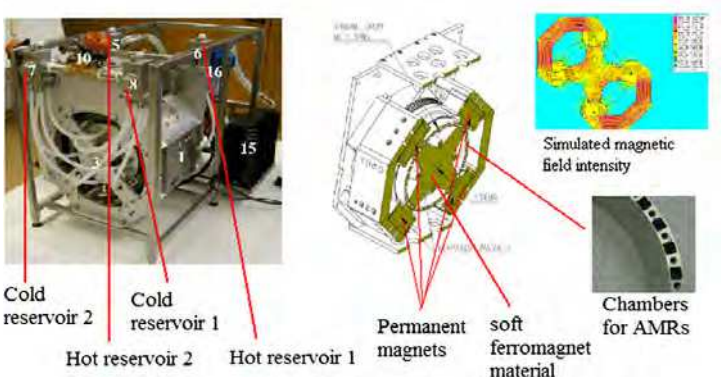

Fig. 15. The rotary magnetic refrigerator developed at the University of Ljubljana in Slovenia (Tusek et al., 2009).

4. Thermal study

Heat exchanges play an important role in magnetic refrigeration systems, both in the cold production cycles, and in the interaction with external environments, including the substance to be cooled. Thus, a thermal study is needed to determine the performance of a magnetic refrigeration system and optimize it. The aim of this section is to focus on the thermal modeling of magnetic AMRR systems.

Most of heat exchanges operating in the magnetic refrigeration are via convection. The convection represents transfer processes performed by the motion of fluids (Bianchi, 2004). In a solid (index 's') in contact, with a fluid (index 'f'), the flow through the wall (index 'w') can be written as:

$$\lambda_s\left(\frac{\partial T}{\partial n}\right)_{ws} = \lambda_f\left(\frac{\partial T}{\partial n}\right)_f = \varphi_p \tag{19}$$

where : n is the normal to the wall and $\lambda\left[W/(m\ K)\right]$ is the thermal conductivity

whereas, the continuity of temperatures can be given by:

$$(T_s)_{wM} = \left(T_f\right)_{wM} \tag{20}$$

where : $(T_s)_{wM}$ is the temperature of the solid at a point 'M' of the wall and $\left(T_f\right)_{wM}$ represents the temperature of the fluid at this point.

According to Newton, there is a linear relationship between the density of heat flow φ and temperature difference $\Delta T = T_s - T_f$ between the solid (T_s) and the fluid (T_f):

$$\varphi = h\Delta T = h\left(T_s - T_f\right) \tag{21}$$

where: $h\left[W/Km^2\right]$ represents the coefficient of heat transfer by convection or simply the convection coefficient.

Using the first law of thermodynamics, by subtracting the mechanical energy, we get the balance of internal energy that gives us the heat equation governing the temperature field at any point in the domain (Janna, 2000)

$$\rho C_p\left(\frac{\partial T}{\partial t} + \mathrm{V.grad}T\right) = \beta T\left(\frac{\partial p}{\partial T} + \mathrm{V.grad}T\right) + P + \Phi + \lambda\ div\left(\mathrm{grad}T\right) \tag{22}$$

where: $\rho\left[kg/m^3\right]$ is he volume density, $C_p\left[J/(kg\ K)\right]$ is the specific heat, V $[m/s]$ is the velocity of the fluid, p $[Pa]$ is the pressure, β $[1/K]$ is the coefficient of dilatation, Φ $[W]$ is the dissipation function and P $[W]$ is the local thermal power produced or absorbed.

For low viscosity fluids and isochors (Janna, 2000), the energy equation reduces to:

$$\rho.C_p\left(\frac{\partial T}{\partial t} + \mathrm{V.grad}T\right) = P + \lambda\ div\left(\mathrm{grad}T\right) \tag{23}$$

if $a = \lambda / \rho C_p$ is defined as the thermal diffusivity of the fluid, thus :

$$\frac{\partial T}{\partial t} + \mathrm{V.grad}T = \frac{P}{\rho C_p} + a.\Delta T \tag{24}$$

4.1 Application to AMRR

Governing equations for AMRR system have been developed throughout the years with the objective of to analytically or numerically describe the thermal behaviour at specific time and for a given set of boundary conditions. They consist of a system of two equations, one for the fluid and the other for the solid matrix. These equations are derived from the energy balance expression for each phase. Since they are coupled they must be solved simultaneously (Bouchekara, 2008). The model of an AMRR cycle has been developed in (Bouchekara, 2008). Fig. 16 illustrates the concept of an AMRR regenerator modelled using one dimensional (1D) approximation.

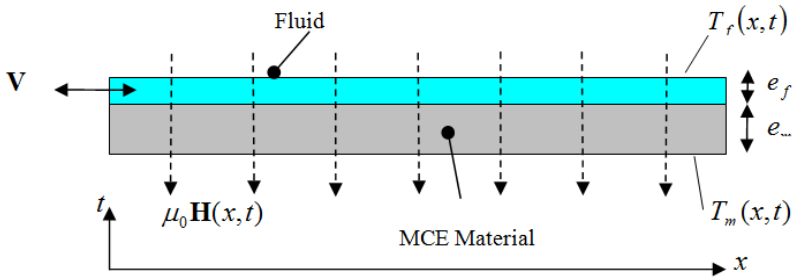

Fig. 16. Conceptual drawing of a 1D AMRR model.

The system of equations given by the energy balance (explained above) for both the magnetocaloric material and the fluid by neglecting the axial conduction (this approximation can be justified for different conditions: low thermal conductivity, very thin plates, etc.) can be summarized by the following system of equations:

$$\begin{cases} m_f C_f\left(T_f\right)\left(\dfrac{\partial T_f}{\partial t} + \dot{d}(t)\dfrac{\partial T_f}{\partial x}\right) = hS\left(T_m - T_f\right) \\ m_m C_m \dfrac{\partial T_m}{\partial t} = hS\left(T_f - T_m\right) \end{cases} \tag{25}$$

To solve this system we use the finite difference method. We use a grid of elements that range from 0 to L for the space and from 0 to τ for the time. Thus, the derivatives with respect to the time are calculated using forward formulas, and those with respect to the space are calculated using backward formulas. This gives a centered discretization scheme. Thus the system (25) becomes:

$$\begin{cases} T_{f_{(i+1,j)}} = A_{f1} T_{f_{(i,j)}} + A_{f2} T_{f_{(i,j-1)}} + A_{f3} T_{m_{(i,j)}} \\ T_{m_{(i+1,j)}} = A_{m1} T_{m_{(i,j)}} + A_{m2} T_{f_{(i,j)}} \end{cases} \tag{26}$$

where: $A_{f1} = \left(1 - \left(\dot{d}(t)\frac{\Delta t}{\Delta x} + \frac{hS}{m_f C_f}\Delta t\right)\right)$, $A_{f2} = \left(\dot{d}(t)\frac{\Delta t}{\Delta x}\right)$, $A_{f3} = \left(\frac{h.S}{m_f C_f}\Delta t\right)$,

$A_{m1=}\left(1 - \frac{h.S}{m_m C_m}\Delta t\right)$ and $A_{m2} = \left(\frac{h.S}{m_m . C_m}\Delta t\right)$

The AMRR model has been implemented using Matlab ® commercial software.

4.2 Results

We will now apply the model developed earlier to a regenerator in the form of plates, as shown in Fig. 17(a). The equivalent cell of the whole regenerator is given in Fig. 17 (b). This cell has the same parameters as the regenerator except the width that is $l_{eq} = N_p l$ (where l_{eq} represents the equivalent width, N_p represents the number of plates and l is the width of one plate).

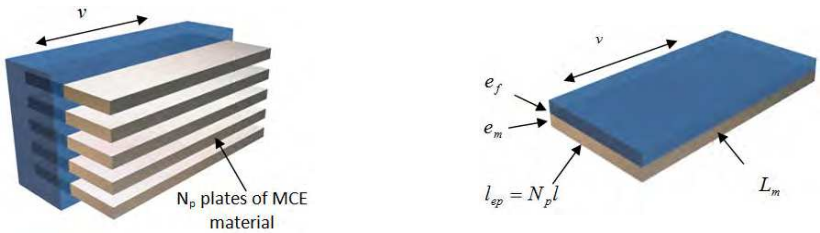

(a) (b)

Fig. 17. (a) A regenerator in the form of plates, (b) Equivalent cell (plate + fluid).

The model parameters (for this simulation case) are shown in Table 2. The magnetocaloric material used is gadolinium, the coolant used is water and the magnetic field is generated by permanent magnets B = 1 T.

Parameters	D(t) [ml/s]	e_m [mm]	e_f [mm]	L_m [mm]	l_{eq} [mm]	ρ [kg/m^3]	C_p [J/(kg K)]	MCE [K]
Values	5	1	0.157	50	573	1000	4185	1.75

Table 2. The parameters used in the simulation.

Fig. 18 (a) shows the temperature evolution of both sides (hot and cold) of the material versus time. After a transient phase, the two curves reach their steady state. In addition, we note that the final value is greater than the initial MCE. From this curve we can extract the evolution of the temperature at the end of each cycle (Fig. 18 (b)). The small delay between the two curves of this figure is due to programming constraints, i.e. the magnetization phase has been introduced (programmed) before the demagnetization phase.

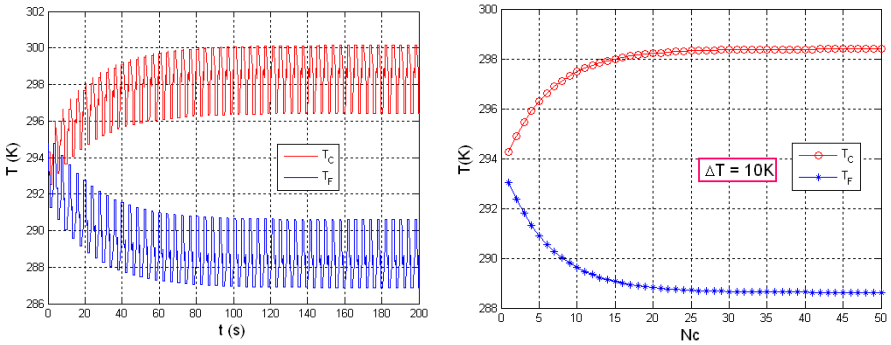

(a) (b)

Fig. 18. Temperature profiles given by the AMRR numerical model.

5. Magnetostatic study

From the definition of the MCE, it is obvious that the performance of a magnetic refrigeration system depends mainly on the efficiency of the MCE material and the strength of the magnetic field. Thus the study of magnetic field sources dedicated to magnetic refrigeration systems is of a paramount importance. In this section we will pay a particular attention to the design of these sources using the finite element method.

The field sources described throughout this section are built with permanent magnets (Neodymium Iron Boron) with a remanent magnetization of $B_r = 1.46$ T and a magnetic permeability of $\mu_r = 1.064$. The MCE material used is gadolinium with isotropic magnetic permeability $\mu_r = 2$. In this study, MCE solid blocks are considered. However, in actuality to ensure a better heat exchange between the MCE material and the exchanging fluid, other forms are considered (plates, powder, etc). The yoke, when it exists, is made of XC10 steel.

5.1 Structure A: monobloc linear system

This first structure is suitable for linear magnetic refrigeration systems with direct cycles. It consists of two magnets (to create the magnetic field), a soft magnetic material yoke (to canalize the magnetic flux) and a block of MCE material (to create the cold) as shown in Fig. 19 (a). The MCE material has a linear alternating movement along the 'y' axis (to achieve magnetization and demagnetization phases). The magnetic characteristics (induction and magnetic force profiles) are shown in Fig. 19 (b) and Fig. 19 (c) while Fig. 19 (d) represents the distribution of the magnetic induction B in Tesla.

5.2 Structure B: Halbach cylider

The structure B is a Halbach cylinder (Fig. 20). It is a magnetized cylinder composed of 'N' segments of ferromagnetic material producing (in the idealized case) an intense magnetic field confined entirely within the cylinder with zero field outside. This second structure can be used in an AMRR system. The MCE material, which can be in the form of plates stacked in a cylinder, is guided by a linear motor or actuator to create the phases of magnetization (material located inside the cylinder) and the demagnetization phase (material located

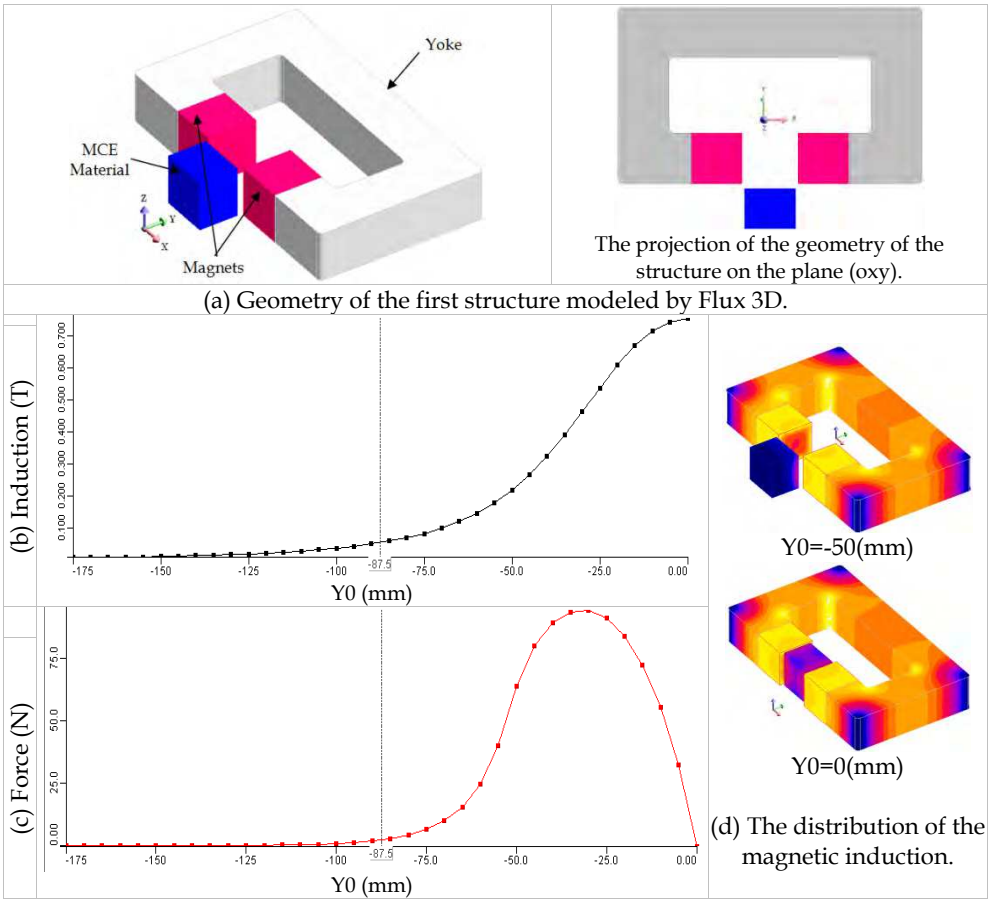

Fig. 19. Geometry and magnetic characteristics of the Structure A.

outside the cylinder). The opposite way works also; i.e. the material remains fixed and the magnet is connected to the linear motor. In this case, the magnetic behavior is the same as in the first case.

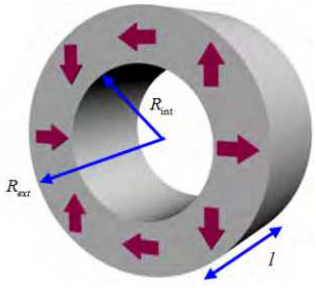

Fig. 20. Cylindre d'Halbach made of eight segments.

We modeled this structure with the commercial software 'Flux 3D'. The parameters used in this simulation are given in Table 3.

Parameters	R_{ext}	R_{int}	R_m	l
Values [mm]	65	25	22	50

Table 3. The dimensions of the Halbach cylinder used in the simulation.

Fig. 21 (a) shows the induction at the center of the material according to the movement. It shows clearly the phases of magnetization and demagnetization produced by this structure. Fig. 21 (b) represents the magnetic forces exerted by the cylinder on the block of MCE material. The distribution of the magnetic induction is shown in Fig. 21 (c).

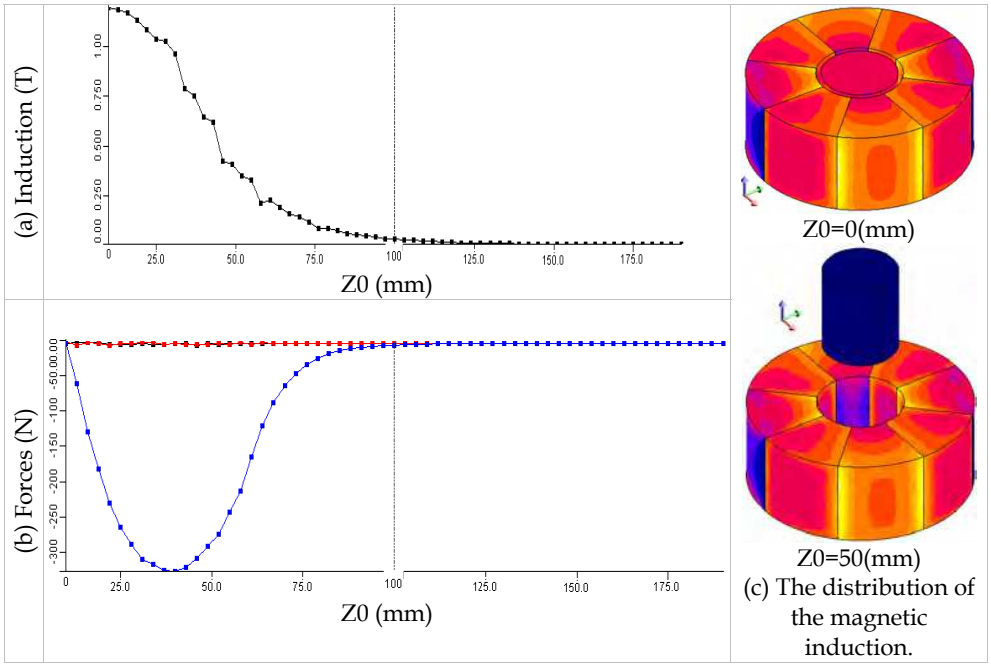

Fig. 21. Magnetic characteristics of the Structure B.

5.2.1 Structure C: double Halbach cylinder

Structure C is a double Halbach cylinder; two cylinders are concentric and have the same number of segments (Fig. 22). Using this structure for magnetic refrigeration systems allows having the phases of magnetization and demagnetization simply by rotating one of the cylinders while the active material remains stationary at the center of the structure. The magnetic field produced at the center is the sum of the two fields produced by each cylinder. When the magnetizations of the first cylinder segments are in the same direction of those of the second cylinder, the magnetic field produced is high and the magnetization phase is achieved (this position is taken as a reference, i.e. $\theta = 0°$). However, when the

magnetizations of the first cylinder are in opposition with those of the second cylinder the magnetic field produced is low ($\theta = 180°$) and the demagnetization phase is achieved.

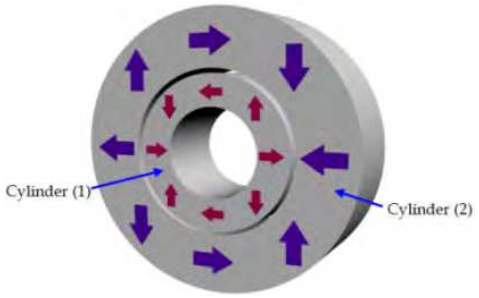

Fig. 22. Double Halbach cylinder (The two cylinders are opposed in this figure).

5.2.2 Structure D: rotating multiblock system

The structure D presented here has a configuration adapted to rotary magnetic refrigeration systems with a direct thermal cycle. It has two magnets to create the field; a yoke of soft material to canalize the magnetic flux and N MCE material blocks for the creation of the cold (Fig. 23). Table 4 below shows the parameter values used in our simulation for the rotating multiblock system.

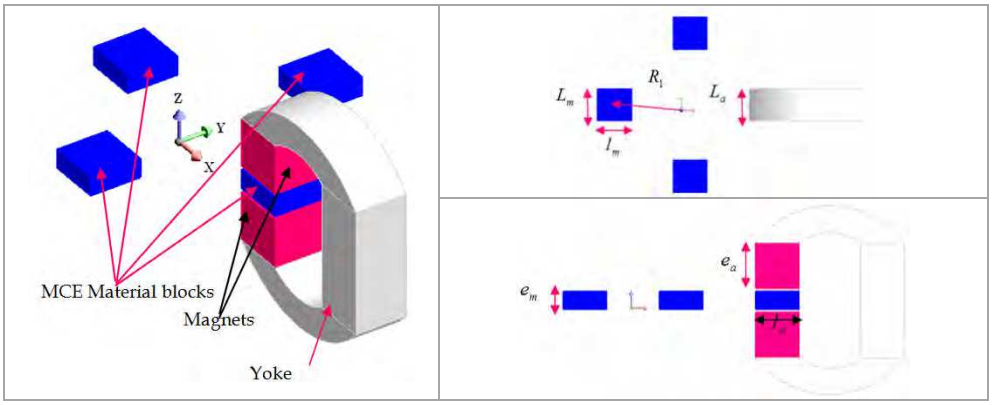

Fig. 23. Geometry of the rotating multiblock system.

Parameters	R_1	l_m	L_m	e_m	l_a	L_a	e_a	e
Values [mm]	100	50	50	20	50	50	20	3

Table 4. The dimensions used in the simulation of the rotating multiblock system.

Fig. 24 (b) shows the induction at the center of a block of material b_1. Fig. 24 (c) and Fig. 24 (d) represent the torque exerted on the blocks and the force exerted on the block b_1, respectively. Fig. 24 (e) represents the distribution of the magnetic induction for two positions $\theta = 0°$ and $\theta = 45°$.

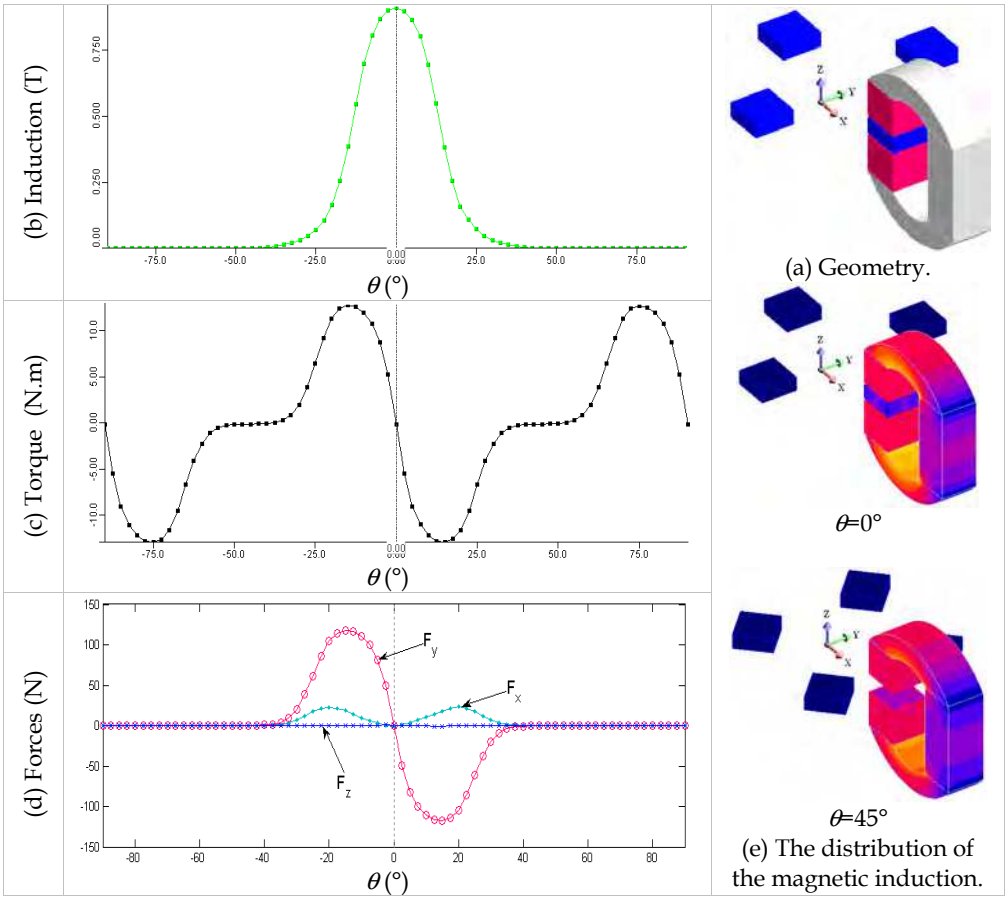

Fig. 24. Magnetic characteristics of the rotating multiblock system.

6. Conclusion

The conventional gas compression refrigerators have been mainly used for refrigeration applications. Generally, such refrigerators are not power-efficient. In addition, gases used in these refrigerators causes harmful effects on the environments. This has led to the development of magnetic refrigeration technology. Over the last decade or so, magnetic refrigeration at room temperature has become the subject of considerable attention. This technology is based on the use of magnetocaloric effect: that is the response of a solid to an applied magnetic field which emerges as a change in its temperature. This technology is

ultimately aimed at developing a standard refrigerator for home use. Unlike conventional refrigerators, magnetic refrigerators are cost-effective and environmentally friendly. Moreover, it is noiseless and power-efficient and requires low maintenance cost and atmospheric pressure besides that its machines are easy to design.

This chapter introduced the magnetic refrigeration technology. It began by providing some essential definitions and provided a detailed review of ten magnetic refrigeration prototypes which are available until now. The operational principle of this technology was explained in depth through the comparison with the conventional one. The chapter then moved on to investigate the study of the magnetocaloric material using the Molecular Field Theory. The thermal study of the magnetic refrigeration process using the finite difference method (FDM) was then explained with providing some useful simulation results. Finally, the magnetic study of magnetic refrigerators using the finite element method (EFM) was presented with some practical results.

7. References

Allab, F. (2008). Conception et réalisation d'un dispositif de réfrigération magnétique basé sur l'effet magnétocalorique et dédié a la climatisation automobile, Thèse de doctorat, Grenoble, *Institut National Polytechnique de Grenoble*.

Bianchi, A.M., Fautrelle, Y., Etay, J. (2004). Transferts thermiques, première édition, *Presses polytechnique et universitaires romandes*, ISBN 2-88074-496-2, Lausanne.

Bjork, R., Bahl, C.R.H., Smith, A., Pryds, N. (2010). Review and comparison of magnet designs for magnetic refrigeration. *International. Journal of Refrigeration*. 33, 437-448.

Bohigas, X., Molins, E., Roig, A., Tejada, J., Zhang, X.X. (2000). Room-temperature magnetic refrigerator using permanent magnets. *IEEE Transactions on Magnetics*, 36 (3), 538-544.

Bouchekara H. (2008). Recherche sur les systèmes de réfrigération magnétique. Modélisation numérique, conception et optimisation, Thèse de doctorat, *Grenoble Institut National Polytechnique*.

Clot, P., Viallet, D., Kedous-Lebouc, A., Fournier, JM., Yonnet, JP., Allab, F. (2003). A magnetic device for active magnetic regeneration refrigeration", *IEEE Transactions on Magnetics*, vol. 39, n° 5, pp. 3349-3351.

Dupuis C. (2009). Matériaux à effet magnétocalorique géant et systèmes de réfrigération magnétique, Thèse de doctorat, Grenoble, *Institut National Polytechnique de Grenoble*.

Engelbrecht, K.L., Nellis, G.F., Klein, S.A., Boeder, A.M. (2005). Modeling Active Magnetic Regenerative Refrigeration Systems, *International Conference on Magnetic Refrigeration at Room Temperature*, Montreux, Switzerland.

Gschneidner, K., Pecharsky, V. (1998). The Giant Magnetocaloric Effect in Gd5 (SixGe1-x4) Materials for Magnetic Refrigeration" *Advances in Cryogenic Engineering*, Plenum Press, New York, pp. 1729.

Huang, W.N., Teng, C.C. (2004). A simple magnetic refrigerator evaluation model. *Journal of Magnetism and Magnetic Materials 282*, pp 311-316.

Janna, W.S. (2000).Engineering Heat Transfer'', ISBN 0-8493-2126-3, CRC Press USA.

Kitanovski, A.P., Egolf, W., Gender, F., Sari, O., Besson, CH. (2005). A Rotary Heat Exchanger Magnetic Refrigerator, *International Conference on Magnetic Refrigeration at Room Temperature*, Montreux, Switzerland.

Lebouc, A., Allab, F., Fournier, J.M., Yonnet, J.P. (2005). Réfrigération magnétique, *[RE 28], Techniques de l'Ingénieurs*.

Muller, C., Bour, L., Vasile, C., (2007). Study of the efficiency of a magnetothermal system according to the permeability of the magnetocaloric material around its Curie temperature. *Proceedings of the Second International Conference on Magnetic Refrigeration at Room Temperature*, Portoroz, Slovenia, pp. 323-330.

Okamura T., Yamada, K., Hirano, N. Nagaya S. (2006). Performance of a roomtemperature rotary magnetic refrigerator'' *International Journal of Refrigeration* 29, 1327-1331.

Okamura T., Yamada, K., Hirano, N. Nagaya S. (2007). Improvement of 100W class room temperature magnetic refrigerator. *Proceedings of the Second International Conference on Magnetic Refrigeration at Room Temperature,* Portoroz, Slovenia, 11-13 April. International Institute of Refrigeration, Paris.

Phan, M.H., Yu, S.C., 2007. Review of the magnetocaloric effect in manganite materials. Journal of Magnetism. and Magnetic. Materials. 308, 325-340.

Tishin, A.M. (1999), Hand Book of Magnetic Material, Vol.12, Ed. Buschow K.H.J., North Holland, Amsterdam.

Tura, A., Rowe, A. (2007). Design and testing of a permanent magnet magnetic refrigerator. *Proceedings of the Second International Conference on Magnetic Refrigeration at Room Temperature*, Portoroz, Slovenia, 11-13 April. International Institute of Refrigeration, Paris, pp. 363-371.

Vasile, C., Muller, C. (2005). A new system for a magnetocaloric refrigerator., *Proceedings of First International Conference on Magnetic Refrigeration at Room Temperature*, Montreux, Switzerland, 27-30 September, International Institute of Refrigeration, Paris, pp. 357-366.

Vasile, C., Muller, C., (2006). Innovative design of a magnetocaloric system. *International Journal of Refrigeration* 29 (8), 1318-1326.

Yu, B., Liu, M., Egolf, P.W., Kitanovski, A., 2010. A review of magnetic refrigerator and heat pump prototypes built before the year 2010. International. Journal of Refrigeration. 33, 1029-1060.

Yu, B.F., Gao, Q., Zhang, B., Meng, X.Z., Chen, Z., 2003. Review on research of room temperature magnetic refrigeration. International. Journal of Refrigeration. 26, 622-636.

Zimm, C., Auringer, J., Boeder, A., Chells, J., Russek, S., Sternberg, A., 2007. Design and initial performance of a magnetic refrigerator with a rotating permanent magnet. *Proceedings of the Second International Conference on Magnetic Refrigeration at Room Temperature*, Portoroz, Slovenia, pp. 341-347.

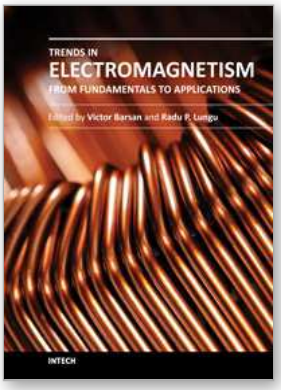

Trends in Electromagnetism - From Fundamentals to Applications
Edited by Dr. Victor Barsan

ISBN 978-953-51-0267-0
Hard cover, 290 pages
Publisher InTech
Published online 23, March, 2012
Published in print edition March, 2012

Among the branches of classical physics, electromagnetism is the domain which experiences the most spectacular development, both in its fundamental and practical aspects. The quantum corrections which generate non-linear terms of the standard Maxwell equations, their specific form in curved spaces, whose predictions can be confronted with the cosmic polarization rotation, or the topological model of electromagnetism, constructed with electromagnetic knots, are significant examples of recent theoretical developments. The similarities of the Sturm-Liouville problems in electromagnetism and quantum mechanics make possible deep analogies between the wave propagation in waveguides, ballistic electron movement in mesoscopic conductors and light propagation on optical fibers, facilitating a better understanding of these topics and fostering the transfer of techniques and results from one domain to another. Industrial applications, like magnetic refrigeration at room temperature or use of metamaterials for antenna couplers and covers, are of utmost practical interest. So, this book offers an interesting and useful reading for a broad category of specialists.

How to reference
In order to correctly reference this scholarly work, feel free to copy and paste the following:

Houssem Rafik El-Hana Bouchekara and Mouaaz Nahas (2012). Magnetic Refrigeration Technology at Room Temperature, Trends in Electromagnetism - From Fundamentals to Applications, Dr. Victor Barsan (Ed.), ISBN: 978-953-51-0267-0, InTech, Available from: http://www.intechopen.com/books/trends-in-electromagnetism-from-fundamentals-to-applications/magnetic-refrigeration-technology-at-room-temperature

INTECH
open science | open minds

InTech Europe
University Campus STeP Ri
Slavka Krautzeka 83/A
51000 Rijeka, Croatia
Phone: +385 (51) 770 447
Fax: +385 (51) 686 166
www.intechopen.com

InTech China
Unit 405, Office Block, Hotel Equatorial Shanghai
No.65, Yan An Road (West), Shanghai, 200040, China
中国上海市延安西路65号上海国际贵都大饭店办公楼405单元
Phone: +86-21-62489820
Fax: +86-21-62489821